Available online at www.sciencedirect.com
ScienceDirect
Trans. Nonferrous Met. Soc. China 21(2011) 1937−1943
Transactions of Nonferrous Metals Society of China
www.tnmsc.cn

Microstructure evolution and mechanical properties of ultrasonic-assisted soldering joints of 2024 aluminum alloys

LI Yuan-xing, ZHAO Wei-wei, LENG Xue-song, FU Qiu-jiao, WANG Lei, YAN Jiu-chun

State Key Laboratory of Advanced Welding Production Technology,
Harbin Institute of Technology, Harbin 150001, China

Received 16 September 2010; accepted 5 January 2011

Abstract: Ultrasonic-assisted soldering of 2024 aluminum alloys using a filler metal of Zn-5Al alloy was investigated at the temperature of 400 °C, which is lower than the solution strengthening temperature of Al-Cu alloys. The ultrasonic vibration with power of 200 W and vibration amplitude of 15 μm at the frequency of 21 kHz was applied on the top samples. The ultrasonic vibration promoted the dissolution of Al elements in the base metal. The reduction of volume fraction of the eutectic phases in the bonds was investigated by increasing ultrasonic vibration time. As the ultrasonic vibration time increased from 3 s to 30 s, the volume fraction of the eutectic phase in the bonds decreased from 12.9% to 0.9%, and the shear strength of the joints was up to 149−153 MPa, increased by 20%. The improvement of the mechanical properties of joints was discussed based on the modulus and hardness of the phases in the bonds and the fracture of the joints.
Key words: 2024 aluminum alloys; brazing; soldering; ultrasonic-assisted soldering; Zn-5Al filler metal

1 Introduction

Joining of heat treatment strengthening Al-Cu alloys is of critical importance in the automotive and aerospace sectors. However, softening and cracking could be hardly ignored during fusion welding [1]. The hardness of heat affected zone (HAZ) of Al-Cu alloys joints could decrease for the loss of the precipitates after fusion welding [2−4]. The cracking of the weld often occurs during the solidification of Al-Cu alloys [5−7]. Generally, the tensile strength of joints with fusion welding can only be up to 60% of that of the base metal. In contrast, friction stir welding (FSW) is a newly developed method for joining 2024 aluminum alloys (a typical Al-Cu alloy) with an ultimate tensile strength being nearly 90% of that of base metal at a lower welding temperature [8−9]. However, it is difficult for FSW method to join the components with complex structures.

Brazing and soldering should be considerable methods to join 2024 aluminum alloys. It is difficult to braze 2024 aluminum alloys with Al-Si system alloys that are generally for brazing aluminum alloys due to the high brazing temperature [10−12]. Accordingly, pure zinc was used as a filler metal to join 3003 aluminum alloys at 475 °C without flux in the argon shielding [13], but the shear strength of joint was very low for the shrink of Zn during solidification. Pure zinc was also used as filler metal to braze A5056 aluminum alloys with ultrasonic vibration at the temperature of 380, 400 and 420 °C, respectively. But the brazed joints did not obtain adequate strength due to the grain boundary segregation of magnesium element [14]. Ultrasonic vibration brazing of A5056 aluminum alloys was also attempted with Zn-Al-Si alloys [15]. However, the grain boundary segregation of silicon element in the filler metal and the formation of voids in the solder filler decreased the tensile strength. In this work, to decrease the soldering temperature, Zn-Al eutectic solder alloys were used to join 2024 aluminum alloys. In order to improve the serviceability temperature of the joints, the volume fraction of the Zn-Al eutectic phase in the bonds was decreased. Simultaneously, the decrease of eutectic phase will also improve the toughness and the shear strength of the joints for the shrinkage voids decreasing. The ultrasonic vibration was used to accelerate the dissolution of Al elements from the base metal to the bond to suppress the formation of the Zn-Al eutectic

Foundation item: Projects (51075104, 50975054) supported by the National Natural Science Foundation of China; Project (2010RFQXG020) supported by the Harbin Excellence Talents Program, China
Corresponding author: LENG Xue-song; Tel: +86-451-86418695; Fax: +86-451-86416186; E-mail: lengxuesong@hit.edu.cn
DOI: 10.1016/S1003-6326(11)60953-9

phase. The reduction of the eutectic phase in the bonds was investigated by increasing ultrasonic vibration time. The relationship between the mechanical properties and the microstructure with different contents of eutectic phase of the joints was discussed. And the micro mechanical properties of phases in the bonds and fracture surface with different applied time of ultrasonic vibration were also studied.

2 Experimental

The base metal used in this study was 2024-T3 aluminum alloy, and Zn-Al alloys were used as filler metal. The chemical compositions of the base metal and the solder are shown in Table 1. The specimen was in size of 50 mm×10 mm×3 mm and polished with abrasive paper and cleaned with acetone before soldering.

Table 1 Chemical compositions of 2024 Al alloys and Zn-Al filler metal (mass fraction, %)

Metal	Cu	Mg	Mn	Fe	Si	Zn	Ti	Ni	Al
Base	4.20	1.50	0.40	0.50	0.50	0.30	0.15	0.10	Bal.
Filler	3.22	0.82	0.91	0.01	0.81	89.30	−	0.05	4.20

The process of ultrasonic-assisted soldering used in this study is illustrated schematically in Fig. 1. The ultrasonic vibration with power of 200 W and vibration amplitude of 15 μm at the frequency of 21 kHz was applied on the lower specimen. Ultrasonic vibration was applied for 3, 10, and 30 s at the temperature of 400 °C, respectively.

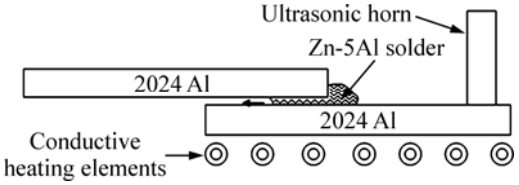

Fig. 1 Schematic of process of ultrasonic-assisted soldering

After joining, the specimens for shear test to determine the joint strength were cut from the joints. Samples for the microstructure observation were also prepared. The microstructure and chemical composition of the joints were examined by an SEM (S4700) equipped with energy dispersive by X-ray spectrometer (EDS). And the volume fraction of the phase was measured by the software analySIS of Olympus GX−71 OM. The shear strength of the bonds was evaluated using a special designed fixture in an electron tension testing machine (Instron 5569). Nano Indenter XP was used to measure hardness and elastic modulus of every phase in the bonds. The depth of the indentation was 500 nm, and the radius of the indenter was 100 nm.

3 Results and discussion

Figure 2 shows the microstructures of the joints with ultrasonic vibration applied for 30 s. The bond zone is mainly composed of 10 μm wide α(Al) layers at both two interfaces of the joints and two kinds of eutectic phases (see Fig. 2(a)). One is striated eutectic phase, which is composed of white η-Zn phase and grey α(Al) phase which grew layer by layer (see Fig. 2(b)). The other is fine eutectic phase, which is composed of η-Zn phase and the grey α(Al) phase. Figure 2(c) shows the magnified image of interface of the bond. And Zn elements diffuse through the boundaries of α(Al) grains. As shown in Fig. 2(d), the interface can get about 8 μm wide Zn-rich layer. Table 2 shows the component of the whole bond and phases, and about 13% Al element is achieved in this bond. The content of fine eutectic phase in the bond is 12.9% measured by software.

Table 2 Chemical compositions of phases and bonds with ultrasonic vibration applied for 3 s (mass fraction, %)

Phase and bond	Al	Zn	Cu	Mg	Ni
Bond	13.0	80	4	0.3	0.7
η-Zn	2.0	98	−	−	−
α(Al)	24.0	76	−	−	−
Fine eutectic	9.7	82	4	4.0	0.4

Figure 3 shows the microstructure of the bonds with ultrasonic vibration applied for 10 s. The width of α(Al) layer increases to about 30 μm. The most of fine eutectic phases change to α(Al) phase and η-Zn phase as shown in Figs. 3(a) and (b). The content of fine eutectic phases decreases to 5.6%. Figures 3(c) and (d) show that the width of the diffusion layer increases to 10 μm. With the diffusion amount of element Zn increasing, the content of element Al in the bond rises to 23% (see Table 3).

Table 3 Chemical compositions of phases and bonds with ultrasonic vibration applied for 10 s (mass fraction, %)

Phase and bond	Al	Zn	Cu	Mg	Ni
Bond	22	74	3	0.6	0.4
η-Zn	3	97	−	−	−
α(Al)	23	77	−	−	−
Fine eutectic	7	82	5	4.0	2.0

Figure 4 shows the microstructure of the joints with ultrasonic vibration applied for 30 s. It is clear that the striated eutectic phases disappear. Instead, the divorced eutectic phases of α(Al) phase and η-Zn phase form grow separately. Moreover, the content of fine eutectic phases decreases sharply, which is only 0.9%. There are several

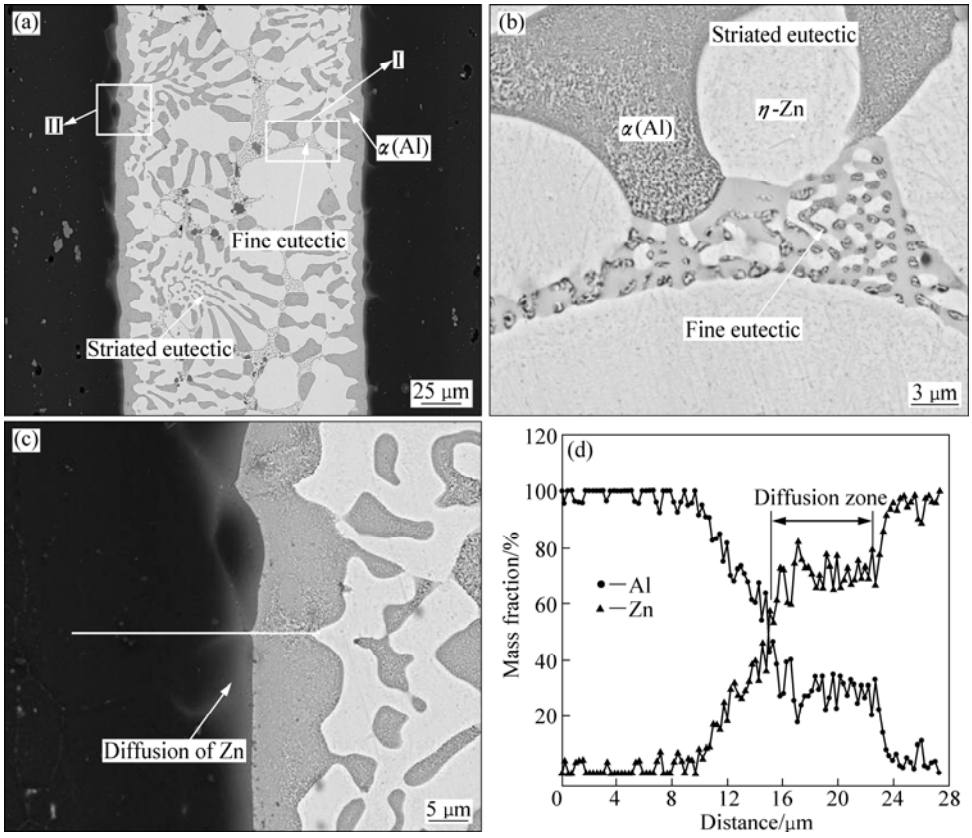

Fig. 2 SEM images of joints with ultrasonic vibration applied at 400 °C for 3 s: (a) Microstructure of bonds; (b) Local magnification of zone I in Fig. 2(a); (c) Local magnification of zone II in Fig. 2(a); (d) Distribution lines of elements Al, Zn at interface in Fig. 2(c)

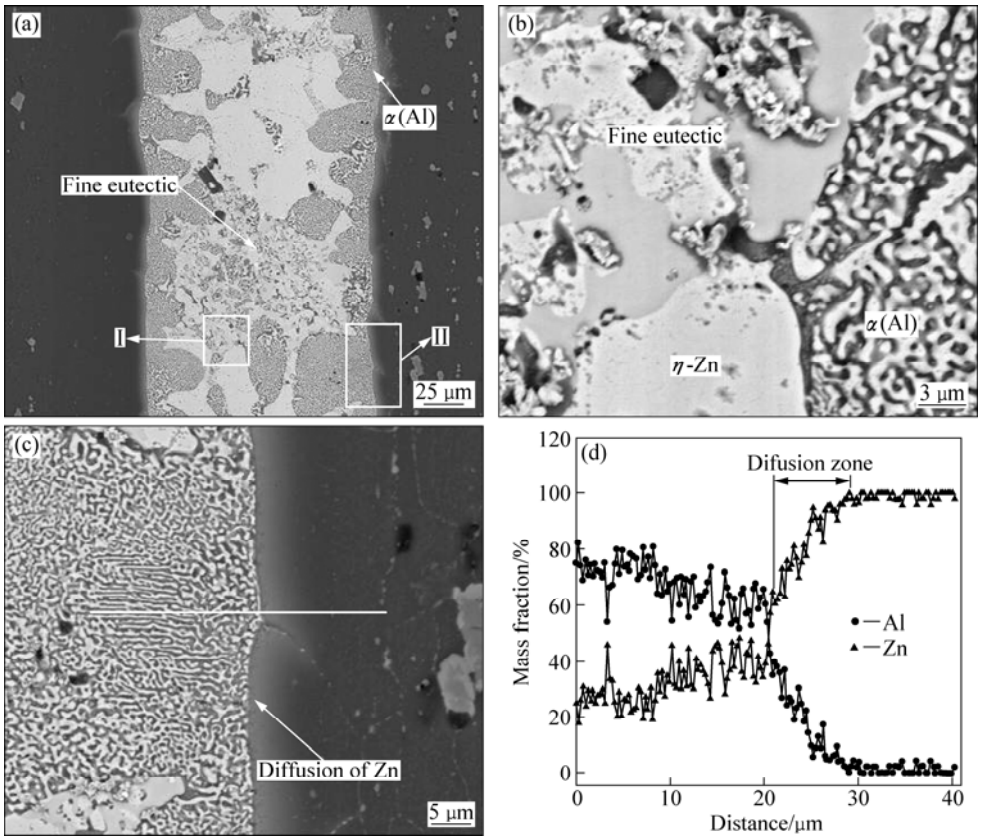

Fig. 3 SEM images of joints with ultrasonic vibration applied at 400 °C for 10 s: (a) Microstructure of bonds; (b) Local magnification of zone I in Fig. 3(a); (c) Local magnification of zone II in Fig. 3(a); (d) Distribution lines of elements Al, Zn at interface in Fig. 3(c)

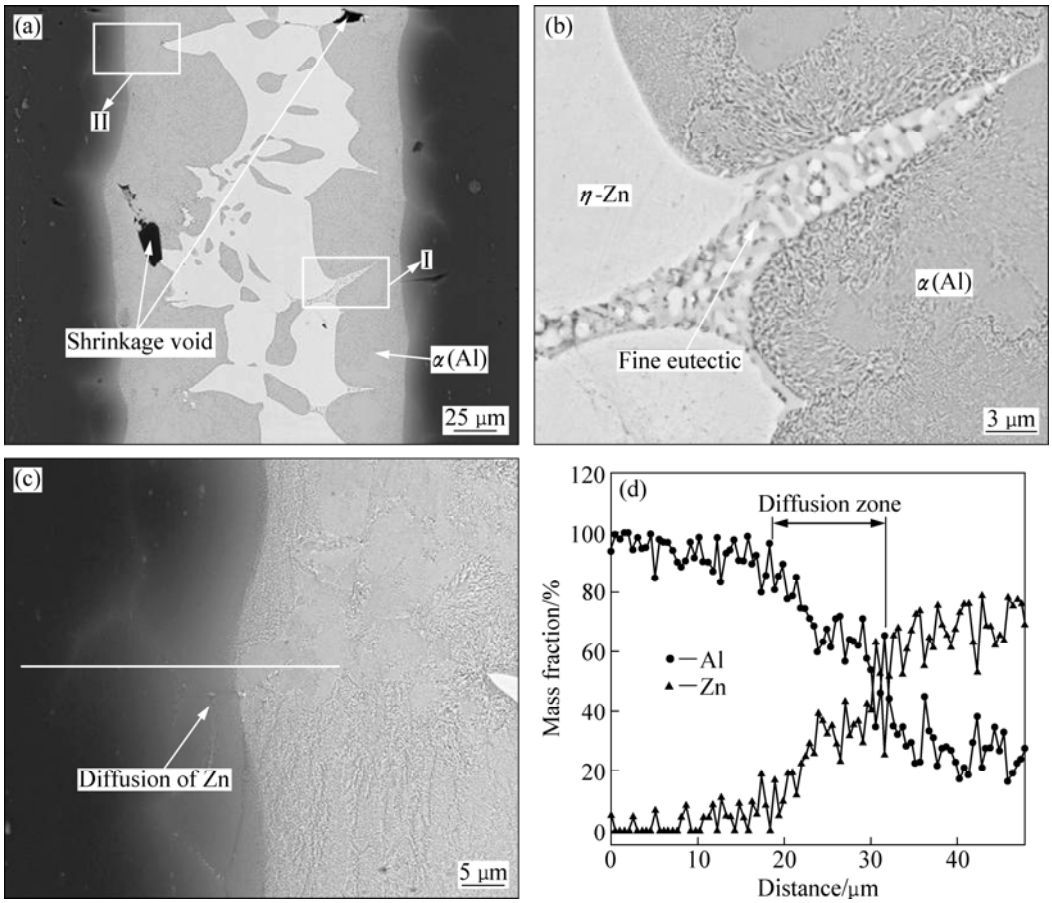

Fig. 4 SEM images of joints of ultrasonic vibration applied at 400 °C for 30 s: (a) Microstructure of bonds; (b) Local magnification of zone I in Fig. 4(a); (c) Local magnification of zone II in Fig. 4(a); (d) Distribution lines of elements Al, Zn at interface in Fig. 4(c)

shrinkage voids near the fine eutectic phase, which are caused by the shrinkage of the liquid in the bond. And the width of α(Al) layer increases to about 60 μm. Figure 4(d) shows that the Zn-rich layer increases to 15 μm in width near the interface with the diffusion amount of element Zn increasing. The composition of the joints are shown in Table 4, and the content of Al element increases to 25% in the bond.

As shown in Tables 2−4, the content of Al element in the bond region increases from 13% to 25% as the ultrasonic vibration time increases from 3 to 30 s, and is even above the ultimate solubility of Al element in Zn at 400 °C (20%，according to Zn-Al binary phase diagram). After ultrasonic vibration applied for 30 s to the 2024 Al, sufficient Al elements will diffuse from the base metal to the bond region. It will make the melting point of the filler metal increase. According to Table 4, the content of Al element in α(Al) is 33%, which is over than the very content of Al at the liquidus line of 400 °C. Therefore, a large amount of α(Al) phases formed at temperature of 400 °C as pre-eutectic phases. Zn element is pushed out of α(Al) phase, forming the divorced eutectic phases finally. At the same time, a large amount of Al element and Zn element in the liquid are almost exhausted, which causes the sharp decline of fine eutectic phase. And the process can be seen from Figs. 3(a)−(b), which shows the formation process of the divorced eutectic phase consumes Al element and Zn element of the liquid, which leads to the fine eutectic phase diminishing.

Table 4 Chemical compositions of phases and bonds with ultrasonic vibration applied for 30 s (mass fraction, %)

Phase and bond	Al	Zn	Cu	Mg	Ni	Fe
Bond	25.0	69	5.00	−	−	1.0
η-Zn	2.0	98	−	−	−	−
α(Al)	33.0	66	0.50	0.5	−	−
Fine eutectic	7.7	69	7.55	5.4	−	2.8

The shear strength of the joints is 126−128 MPa with ultrasonic vibration applied for 3 s, and 149−153 MPa applied for 30 s, increased by 20% for 30 s than that for 3 s.

Figure 5 shows the shear fracture surfaces of the joints with different ultrasonic vibration time. All the fractures of the joints occur in the solder layer. Figure 5(a) shows the typical shear fracture surface of the bond with the ultrasonic vibration applied for 3 s. And the smooth pattern is identified as η-Zn phase by EDS analysis. And

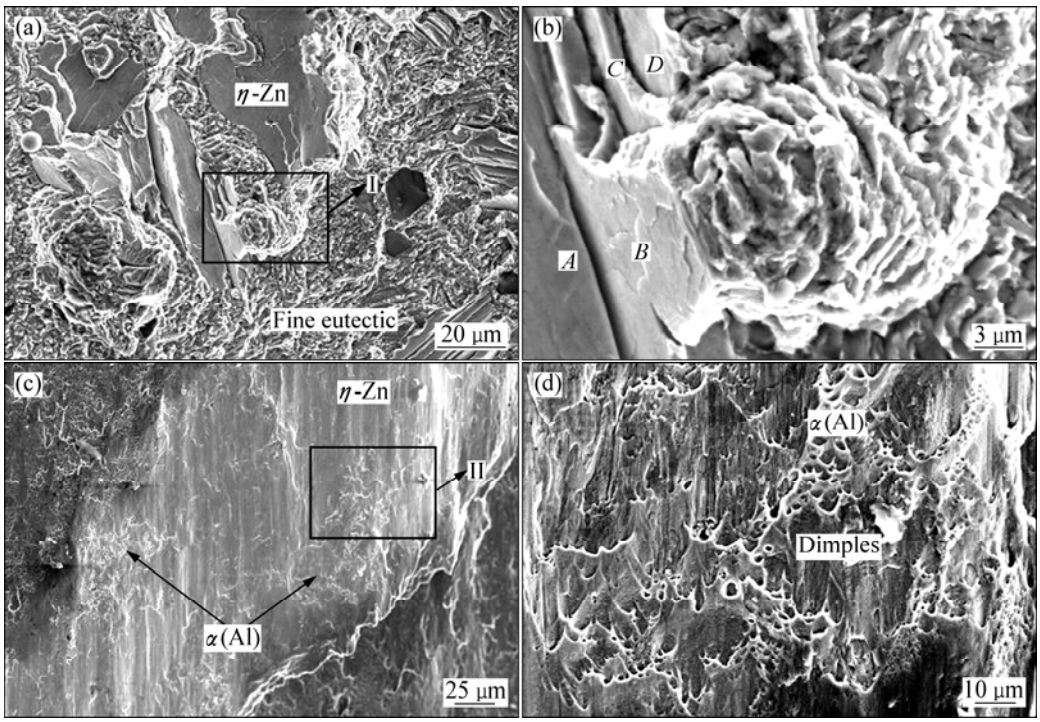

Fig. 5 Shear fracture surfaces with ultrasonic vibration applied for different time: (a) Applied for 3 s; (b) Magnification of zone I in Fig. 5(a); (c) Applied for 30 s; (b) Magnification of zone II in Fig. 5(a)

the other rough pattern is identified as the fine eutectic phase. Figure 5(b) shows the magnification image of zone I in Fig. 5(a). It shows that several layers bond and every layer (*A*, *B*, *C*, and *D*) is identified as *η*-Zn phase by EDS analysis. Compared with Fig. 2(a), it can be inferred that the *η*-Zn phase is composed of the striated eutectic (see Fig. 2(b)). But the other phase which is composed of the striated eutectic *α*(Al) phases is not found on the fracture surface in Fig. 5(b). Figure 5(c) shows the fracture surface of the bonds with ultrasonic vibration applied for 30 s. It is composed of *η*-Zn phase and *α*(Al) phase identified by energy spectrum analysis. Figure 5(d) shows the dimples of the fracture, which is identified as *α*(Al).

Table 5 shows the elastic modulus and nano-hardness of the phases in the bond with ultrasonic vibration applied for 3 s. It suggests that the fine eutectic phase has the largest elastic modulus in the bond, which is 114−117 GPa. And its hardness is also the largest, which is 2.0−2.1 GPa. This indicates that fine eutectic phase is the last one to deformation. And the elastic modulus of *η*-Zn phase is the smallest, only 89−94 GPa, which is about 20 GPa lower than that of fine eutectic phase. And its hardness is also the smallest, only 1.4 GPa. This indicates that *η*-Zn phase has a large plastic deformation under the force. That is why *α*(Al) phases are not seen on the fracture surface (Fig. 5(b)). They are folded by the *η*-Zn phase layers for the poor deformation ability. Table 6 shows the elastic modulus and the hardness of the phases in the joint with ultrasonic vibration applied for 30 s. The results show that the modulus and the hardness of *α*(Al) phase are a little higher than those of *η*-Zn phase. Compared with the data of the joint with ultrasonic vibration applied for 3 s, the modulus and hardness of phases only change a little. This indicates that the reason of different fracture and shear strength is not due to the change of the modulus and hardness of phases.

It should be noticed that there are two main differences of the two joints. The first one is the sharp decline of the fine eutectic phase of the bond. According to the results of the nano-hardness and modulus tested, the *η*-Zn phase has the larger ductility than the fine eutectic phase. So the joints with high content of fine

Table 5 Nano-hardness and modulus of phases in bonds with ultrasonic vibration applied for 3 s

Phase	Elastic modulus/GPa	Hardness/GPa
Fine eutectic	114−117	2.0−2.1
α(Al)	106−108	1.5−1.56
η-Zn	89−94	1.39−1.43

Table 6 Nano-hardness and modulus of phases in bonds with ultrasonic vibration applied for 30 s

Phase	Elastic modulus/GPa	Hardness/GPa
α(Al)	95−102	1.7−2.2
η-Zn	88−94	1.5−1.6

eutectic phase trend to crack easily for the brittle phase. According to the measured results, the content of fine eutectic phase of the joints with ultrasonic vibration applied for 3 s is 12.9%, much higher than 0.9% of the joints for 30 s.

Secondly, the interface between the fine eutectic phase and the striated eutectic phase is flat, which can be seen from the bond with ultrasonic vibration applied for 3 s (see Fig. 2(b)). As the shear force loads on, η-Zn phase deforms firstly for its low elastic modulus and hardness, while the fine eutectic phase is hard to deform. So the crack generated at the grain boundary between the η-Zn phase and fine eutectic phase. With the shear force loading on, all the η-Zn phase has a large deformation, more and more cracks occur at the interface between η-Zn phase and fine eutectic phase. Until the interface is completely torn, some cracks cross the fine eutectic phases. And the flat fracture surface of η-Zn phase and the rough surface of fine eutectic phase are formed as shown in Fig. 5(a). In the whole process, α(Al) phases deform hardly, so it is folded by the two layers of η-Zn phases beside it. That is why it cannot be seen in the fracture of Fig. 5(b). The interface between η-Zn phases and α(Al) phases of the joint with ultrasonic vibration applied for 30 s is rough as shown in Fig. 4(a). When the shear force loads on the bond with ultrasonic vibration applied for 30 s, both η-Zn phase and α(Al) phase have a deformation, and the deformation of η-Zn phase is larger than that of α(Al) phase. The rough interface between the two phases suppresses the cracks of interface to some extent.

4 Conclusions

1) The ultrasonic vibration with power of 200 W and vibration amplitude of 15 μm at the frequency of 21 kHz was applied on 2024 aluminum alloys with Zn-5Al filler metal at 400 °C. It was found that the ultrasonic vibration can promote the dissolution of Al elements in the base metal. The content of Al element in the bonds increases from 13% to 25% with the ultrasonic vibration time increasing from 3 to 30 s.

2) The microstructure evolution of bonds with the ultrasonic vibration time increasing was investigated. The typical bonds are mainly composed of the striated eutectic phases and fine eutectic phases with the ultrasonic vibration time of 3 s. The striated eutectic phases change completely into devoiced eutectic phases of α(Al) phase and η-Zn phase in the bonds for 30 s. And the volume fraction of the fine eutectic phases declines from 12.9% to 0.9%.

3) The shear strength of joints with ultrasonic vibration applied for 30 s is 149−153 MPa, which is 20% higher than that of the joints for 3 s. The improvement of shear strength of the joints is mainly caused by the evolution of the microstructure and the sharp decline of the volume fraction of the eutectic phases.

References

[1] GHAINI M F, SHEIKHI M, TORKAMANY M J, SABBAGHZADEH J. The relation between liquation and solidification cracks in pulsed laser welding of 2024 aluminium alloy [J]. Materials Science and Engineering A, 2009, 519: 167−171.

[2] WANG S C, STARINK M J, GAO N. Precipitation hardening in Al-Cu-Mg alloys revisited [J]. Scripta Materialia, 2006, 54(2): 287−291.

[3] BDAVIS S, LI Y, MURR L E BROWN D, MCCLURE J C. Low-temperature friction-stir welding of 2024 aluminum [J]. Scripta Materialia, 1999, 41(8): 809−815.

[4] OWEN R A, PRESTON R V, WITHERS P J, SHERCLIFF H R, WEBSTER P J. Neutron and synchrotron measurements of residual strain in TIG welded aluminium alloy 2024 [J]. Materials Science and Engineering A, 2003, 346: 159−167.

[5] WEETER L. Technological advances in aluminum laser welding [J]. Practical Welding Today, 1998, 2 (1): 56−57.

[6] ALI A, AN X, RODOPOULOS C, BROWN A M W, HARA P O, LEVERS A, GARDINER S. The effect of controlled shot peening on the fatigue behavior of 2024-T3 aluminium friction stir welds [J]. International Journal of Fatigue, 2007, 29: 1531−1545.

[7] XUE Song-bai, DONG Jian, LÜ Xiao-chun, QIAN Yi-yu. Brazing technology of LY12 Al-alloy at middle temperature [J]. Transactions of the China Welding Institution, 2003, 24(3): 21−22. (in Chinese)

[8] ALI A, BROWN M W, RODOPOULOS A. Modeling of crack coalescence in 2024-T351 Al alloy friction stir welded joints [J]. International Journal of Fatigue, 2008, 30: 2030−2043.

[9] LIU Ke-wen, XING Li, KE Li-ming. Microstructures and properties of friction stir spot welding joints for LY12 aluminum alloy [J]. The Chinese Journal of Nonferrous Metals, 2008, 18(2): 288−293. (in Chinese)

[10] SHUKLA A K, BAESLACK W A. Process-property relationships and microstructure evolution in friction stir welded thin sheet 2024-T3 aluminum alloy [C]//Proceedings of 7th International Conference on Trends in Welding Research. Georgia: ASM International, 2006: 377−382.

[11] TSAO L C, CHIANG M J, LIN W H, CHENG M D, CHUANG T H. Effects of zinc additions on the microstructure and melting temperatures of Al-Si-Cu filler metals [J]. Materials Characterization, 2002, 48: 341−346.

[12] TSAO L C, CHIANG M J, LIN W H, TSAI T C, WU C S. Development of a low-melting-point filler metal for brazing aluminum alloys [J]. Metallurgical and Materials Transaction A, 2000, 31(10): 2239−2245.

[13] MOVAHEDI M, KOKABI A H, MADDSH H R. An investigation on the soldering of Al 3003/Zn sheets [J]. Materials Characterization, 2009, 60: 441−446.

[14] WATANABE T, TANAKA Y, YANAGISAWA A, ONUMA S. Joining process and the effect of surface finishing in soldering aluminum [J]. Quarterly Journal of Japan Welding Society Weld Soc, 1992, 10: 470−476.

[15] WATANABE T, YANAGISAWA A, FURUKAWA A, ONUMA S. Soldering of Al-Mg alloy with the aid of ultrasonic vibration [J]. Quarterly Journal of Japan Welding Society Weld Soc, 1993, 11(4): 484−489.

2024 铝合金超声辅助钎焊接头的微观组织演变及力学性能

李远星，赵维巍，冷雪松，付秋娇，王 雷，闫久春

哈尔滨工业大学 现代焊接生产技术国家重点实验室，哈尔滨 150001

摘 要：对低温下采用 Zn-5Al 钎料超声辅助钎焊 2024 铝合金进行研究。在温度为 400 °C 时，采用功率为 200 W、振幅为 15 μm、频率为 21 kHz 的超声对试样实施连接。采用超声波来加速 Al 从母材到焊缝的溶解，从而改变接头的微观组织。同时，通过增加超声时间来降低接头中共晶组织的含量。当超声振动时间从 3 s 增加到 30 s 时，焊缝中共晶相的含量从 12.9%减少到 0.9%剪切强度提高了 20%，并且，当超声振动时间为 30 s 时，接头的剪切强度达到最大为 149−153 MPa。为了研究接头力学性能的变化，测试了接头中各相的弹性模量和硬度，同时分析了不同超声振动时间下的接头断口形貌。

关键词：2024 铝合金；钎焊；软钎焊；超声辅助钎焊；Zn-5Al 钎料

(Edited by LI Xiang-qun)